Pressure-induced modifications of the magnetic order in the spin-chain compound $Ca_3Co_2O_6$

D. P. Kozlenko,[1,*] N. T. Dang,[2,†] N. O. Golosova,[1] S. E. Kichanov,[1] E. V. Lukin,[1] P. J. Lampen Kelley,[3] E. M. Clements,[3] K. V. Glazyrin,[4] S. H. Jabarov,[5] T. L. Phan,[6] B. N. Savenko,[1] H. Srikanth,[3] and M. H. Phan[3,‡]

[1]*Frank Laboratory of Neutron Physics, Joint Institute for Nuclear Research, 141980 Dubna, Russia*

[2]*Institute of Research and Development, Duy Tan University, 550000 Da Nang, Vietnam*

[3]*Department of Physics, University of South Florida, Tampa, Florida 33620, USA*

[4]*Photon Sciences, Deutsches Elektronen Synchrotron, D-22607 Hamburg, Germany*

[5]*Institute of Physics, Azerbaijan National Academy of Sciences, Baku, Azerbaijan*

[6]*Department of Physics and Oxide Research Center, Hankuk University of Foreign Studies, Yongin, South Korea*

(Received 19 June 2018; revised manuscript received 2 October 2018; published 19 October 2018)

The structural and magnetic properties of the $Ca_3Co_2O_6$ spin-chain compound have been studied by means of neutron and x-ray powder diffraction at pressures up to 6.8 and 32 GPa, respectively. A suppression of the initial spin-density wave state ($T_N = 25$ K) and stabilization of the collinear commensurate antiferromagnetic (AFM) state at high pressures ($T_{NC} = 26$ K at $P = 2.1$ GPa) were observed. The pressure behavior of the competing intra- and interchain magnetic interactions was analyzed on the basis of obtained structural data and their role in the formation of the magnetic phase diagram is discussed. The pressure behavior of the Néel temperature of the commensurate AFM phase was evaluated within the mean field theory approach and a good agreement with the experimental value $dT_{NC}/dP = 0.65$ K/GPa was obtained.

DOI: 10.1103/PhysRevB.98.134435

I. INTRODUCTION

The low-dimensional spin-chain magnetic systems exhibit a rich variety of challenging physical phenomena like quantum critical point, Bose-Einstein condensation, Haldane gap excitations, exotic magnetic ground states, formation of magnetization plateaus in external magnetic fields, and multiferroicity, which are at the current focus of extensive research [1–8].

Among the spin-chain systems an interesting model compound, demonstrating a number of the above-mentioned phenomena, is $Ca_3Co_2O_6$. In its rhombohedral crystal structure with $R\bar{3}c$ symmetry (Fig. 1), quasi-one-dimensional Ising chains are formed due to alternating arrangement of face-sharing $Co(1)O_6$ octahedra and $Co(2)O_6$ trigonal prisms along the c axis, which are arranged in a triangular lattice in the ab plane [9]. Due to the different crystalline electric-field splittings, the $Co^{3+}(1)$ and $Co^{3+}(2)$ ions with the octahedral and the triangular base prism oxygen coordination have low-spin (LS, $S = 0$) and high-spin (HS, $S = 2$) states, respectively.

The ferromagnetic (FM) intrachain interactions are rather strong, $J_1 \approx 25$ K, while antiferromagnetic (AFM) interchain ones $J_2 \approx J_3 \approx 1$ K (Fig. 1) are more than an order of magnitude weaker [10–12]. A combination of low dimensionality and geometric frustration on the triangular lattice leads to unexpectedly complex magnetic behavior of $Ca_3Co_2O_6$, debated for a long time [13–19]. According to the latest results, below the Néel temperature $T_N = 25$ K the incommensurate amplitude modulated spin-density wave (SDW) magnetic state with a propagation vector $q_{sdw} = (0, 0, 1.01)$ is formed. At lower temperature $T_{N1} \approx 10$ K, the incommensurate magnetic order transforms partially to the commensurate AFM state with a propagation vector $q_{caf} = (0.5, -0.5, 1)$ [15,16]. This transformation evolves slowly in time and its realization depends strongly on the temperature variation rate. The presence of short-range magnetic correlations at low temperatures was also observed [15]. In the external fields several magnetization plateaus were detected in $Ca_3Co_2O_6$, associated with the formation of ferri- and ferromagnetic states [12,14,20]. While novel magnetoelectric phenomena were observed in parent $Ca_3Co_2O_6$ [21], its substituted compounds $Ca_3Co_{2-x}Mn_xO_6$ ($x \sim 1$) are improper multiferroics with a notable ferroelectric polarization [22].

An appearance of competing magnetic states in $Ca_3Co_2O_6$ results from a delicate balance of intra- and interchain magnetic interactions realized on the geometrically frustrated triangular lattice, which can be tuned by variation of external parameters like temperature and magnetic field. Further important insight in exploration of particular factors responsible for complex physical phenomena observed in $Ca_3Co_2O_6$ and underlying structure-properties relationships can be achieved by high-pressure studies, mediating competing interactions by modifications of interatomic distances and angles. In this paper, the crystal and magnetic structures of $Ca_3Co_2O_6$ have been studied by means of x-ray and neutron powder diffraction at high pressures up to 32 and 6.8 GPa, respectively.

II. EXPERIMENTAL DETAILS

The polycrystalline $Ca_3Co_2O_6$ samples were synthesized by a conventional sol-gel method. Stoichiometric amounts of

*denk@nf.jinr.ru
†dangtoan2107@gmail.com
‡phanm@usf.edu

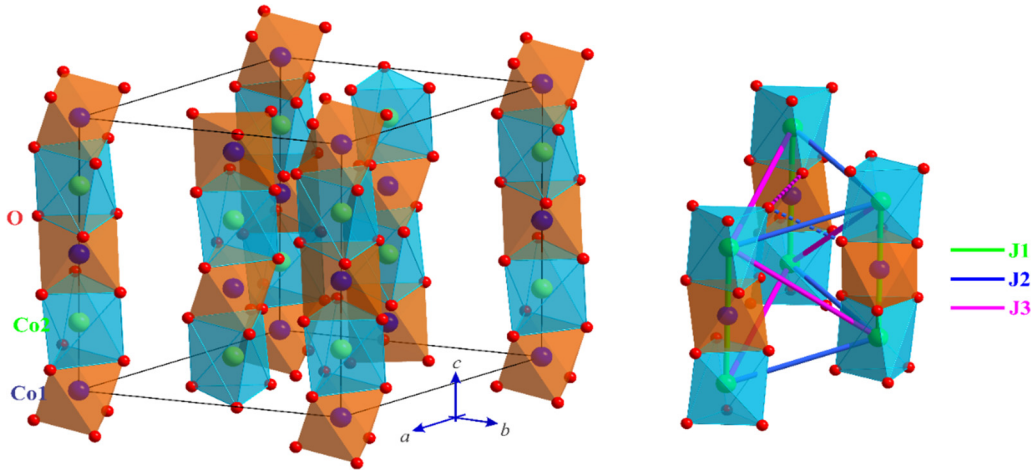

FIG. 1. The rhombohedral crystal structure of $Ca_3Co_2O_6$. The paths of the intra- (J_1) and interchain (J_2, J_3) interactions are shown.

$Co(NO_3)_2 \cdot 6H_2O$ and $Ca(NO_3)_2 \cdot 4H_2O$ were dissolved in deionized water in appropriate molar ratios under stirring, and citric acid was added until a metal nitrate–citric acid ratio of 1:4 was achieved. The solution was stirred at 80 °C for 9 h while the solvent slowly evaporated to form gel. The gel was transferred to a hot plate and the temperature was increased until a porous black powder formed at 250 °C and the resulting powder was ground and calcined at 400 °C overnight to remove organic materials after which high-temperature treatments were performed in a tube furnace under an oxygen atmosphere to form the single $Ca_3Co_2O_6$ phase [23].

The angle-dispersive x-ray powder-diffraction patterns at pressures up to 32 GPa and ambient temperature were measured at the Extreme Conditions Beamline [24]. (P02.2, PETRA III, DESY, Germany) using the wavelength $\lambda = 0.29118$ Å. The BX90-type diamond anvil cell [25] was used in the experiments. The diamonds with culets of 300 μm were used. The sample was loaded into the hole of the 150-μm diameter made in the Re gasket indented to about 25-μm thickness. Neon gas loaded under pressure of $P \sim 0.15$ GPa was used as a pressure transmitting medium. The two-dimensional x-ray-diffraction (XRD) images were converted to the one-dimensional diffraction patterns using the FIT2D program [26].

The neutron powder-diffraction measurements at pressures up to 6.8 GPa were performed at selected temperatures in the range 4–290 K with the DN-12 and DN-6 diffractometers (IBR-2 pulsed reactor, JINR, Russia) [27]. The sample with a volume of about $2mm^3$ was loaded into the sapphire anvil high pressure cells [28] with culets of 4 mm. The spherical holes with a diameter of 2 mm were drilled at the culet centers for the quasihydrostatic pressure distribution at the sample surface. The diffraction patterns were collected at the scattering angles of 90 and 45° with the resolution $\Delta d/d = 0.015$ and 0.022, respectively. The pressure inside the sapphire and diamond anvil cells was measured using the ruby fluorescence technique. The pressure gradients were less than 10% with respect to average pressure value. The x-ray and neutron powder-diffraction patterns were analyzed by the Rietveld method using the FULLPROF program [29].

III. RESULTS AND DISCUSSION

A. X-ray diffraction

The XRD patterns of $Ca_3Co_2O_6$ obtained at selected pressures and ambient temperature are shown in Fig. 2. In the whole studied pressure range they correspond to the initial rhombohedral structure of $R\bar{3}c$ symmetry. The lattice-parameter values determined at ambient conditions, $a = 9.0663(3)$Å and $c = 10.372(4)$Å (in hexagonal setting), are consistent with earlier studies [9,12].

The lattice compression of $Ca_3Co_2O_6$ (Fig. 3) demonstrates substantial anisotropy with an average compressibility $[k_i = -(1/a_{i0})(da_i/dP)_T]$ of the a lattice parameter, $k_a = 0.0072$ GPa^{-1}, about 40% larger in comparison with the c one, $k_c = 0.0052$ GPa^{-1}. This is a consequence of the chain-like character of the crystal structure, resulting in the reduced atomic density within the ab planes. The volume compressibility data were fitted by the third-order Birch-Murnaghan

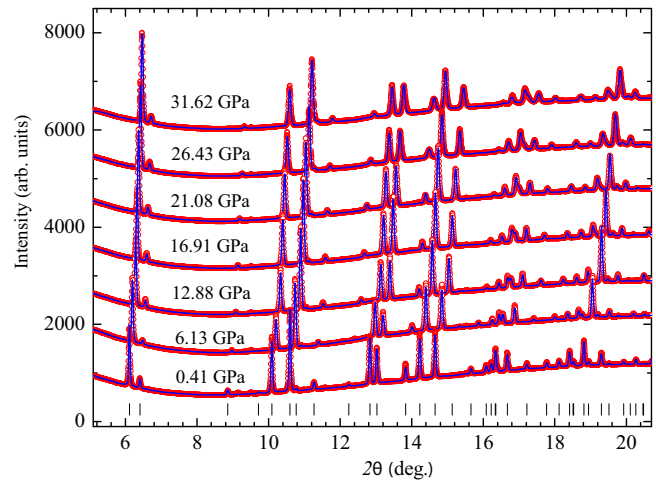

FIG. 2. X-ray-diffraction patterns of $Ca_3Co_2O_6$ measured at selected pressures and ambient temperature, and refined by the Rietveld method. Experimental points and calculated profiles are shown. Tick-marks at the bottom represent the calculated positions of diffraction peaks at $P = 0.41$ GPa. The weak peaks at $2\theta \approx 9.15$ and 9.50° are the background lines.

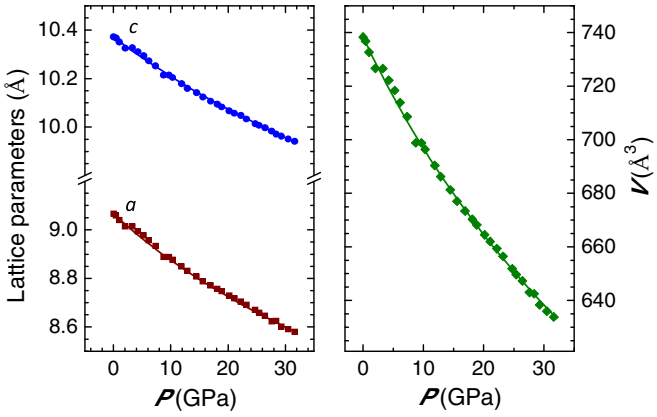

FIG. 3. The pressure dependences of lattice parameters and unit-cell volume of $Ca_3Co_2O_6$ and their interpolations using the Birch-Murnaghan equation of state.

equation of state [30]:

$$P = \frac{3}{2}B_0(x^{-7/3}\text{-}x^{-5/3})\left[1 + \frac{3}{4}(B' - 4)(x^{-2/3} - 1)\right], \quad (1)$$

where $x = V/V_0$ is the relative volume change, V_0 is the unit-cell volume at ambient pressure, and B_0 and B' are the bulk modulus $[B_0 = -V(dP/dV)_T]$ and its pressure derivative $[B' = (dB_0/dP)_T]$.

The obtained values of $B_0 = 154(5)$ GPa and $B' = 4.0(5)$ are comparable with those of the perovskitelike $LaCoO_3$ compound ($B_0 = 165$ GPa) [31], having Co^{3+} ions in the octahedral oxygen coordination only.

B. Neutron diffraction

The neutron-diffraction patterns of $Ca_3Co_2O_6$, measured at selected pressures up to 6.8 GPa and low temperatures, are shown in Fig. 4. At ambient pressure below $T_N = 25$ K an appearance of magnetic peaks located at d_{hkl} positions of 3.90, 3.41, 3.10, and 2.98 Å was observed. The data analysis has shown that these peaks correspond to formation of the incommensurate SDW long-range AFM order of the Co2 spins oriented along the c axis with a propagation vector $q = (0, 0, q_z \approx 1.01)$, in accordance with Ref. [16]. The value of the ordered magnetic moment obtained at $T = 20$ K, $m_{Co2} = 4.1(1)\mu_B$, is consistent with those obtained in previous neutron-diffraction studies for powdered ($3.0\mu_B$) and single-crystal ($5.0\mu_B$) samples [13,32] as well as the expected spin-only value for the HS state of Co^{3+} ions, $S = 2$ ($4.89\mu_B$).

The intensity of magnetic peaks associated with the SDW phase first increased on cooling down to 15 K and reduced sharply at lower temperatures (Fig. 5). A more detailed inspection of the most intense magnetic peak $(2, -2, 1 - q_z)$ located at 3.90 Å ($q = 1.61$ Å^{-1}) revealed an additional broad component, slightly shifted to lower d spacing (higher q values), the intensity of which, in contrast, demonstrated a growing on cooling below $T = 15$ K. Such a behavior may be related to a presence of the short-range ordered magnetic phase, the volume fraction of which increases at the expense of the gradually suppressed SDW phase at low temperature, as observed previously [32].

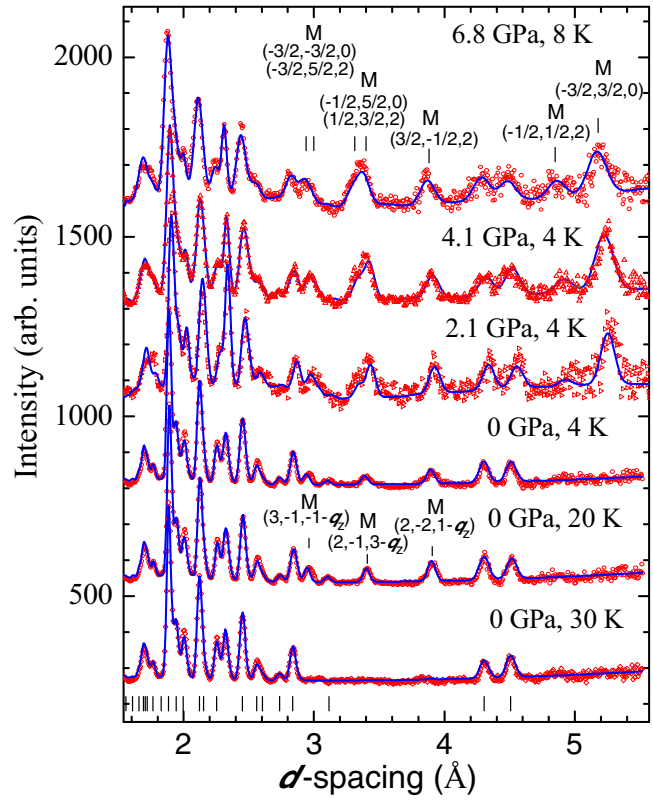

FIG. 4. Neutron-diffraction patterns of $Ca_3Co_2O_6$, measured at selected pressures up to 6.8 GPa and low temperatures, and processed by the Rietveld method. The neighboring patterns are shifted along the vertical axis by 250 units. The experimental points and calculated profiles are shown. The ticks below represent the calculated positions of the structural peaks for $P = 0$ GPa, $T = 30$ K. The positions of the characteristic magnetic peaks of the SDW phase at ambient pressure and commensurate AFM phase at high pressure are marked as "M" and relevant peak indices are given.

The magnetic correlation length in the SRO phase, evaluated by the Selyakov-Scherrer formula ($\xi \approx 2\pi/\Delta q_{sro}$) using the full width at half maximum (Δq_{sro}) of the relevant magnetic peak in the reciprocal q space, is $\xi = 128(7)$Å and weakly temperature dependent. In this approach, the exponentially decaying character of the spin correlation function is assumed. This value is comparable with one of 180 Å in the ab plane obtained in Ref. [32]. No time-dependent transformation into the commensurate AFM phase was observed at temperatures below 10 K, although characteristic measurement times of about 4 h at each temperature were comparable with those in Ref. [16].

At high pressure $P = 2.1$ GPa and temperatures below 30 K an appearance of new magnetic peak at $d_{hkl} = 5.21$Å, as well as splitting and redistribution of the intensity of the magnetic peaks located at $d_{hkl} \approx 3.41$ and 2.98 Å, were observed, evidencing the magnetic phase transformation. The model of the collinear antiferromagnetic order with $q_{caf} = (0.5, -0.5, 1)$ provides a good description of the experimental data. The intensities of all the observed diffraction peaks can be fitted well with a single commensurate AFM magnetic phase, implying a suppression of the initial SDW phase.

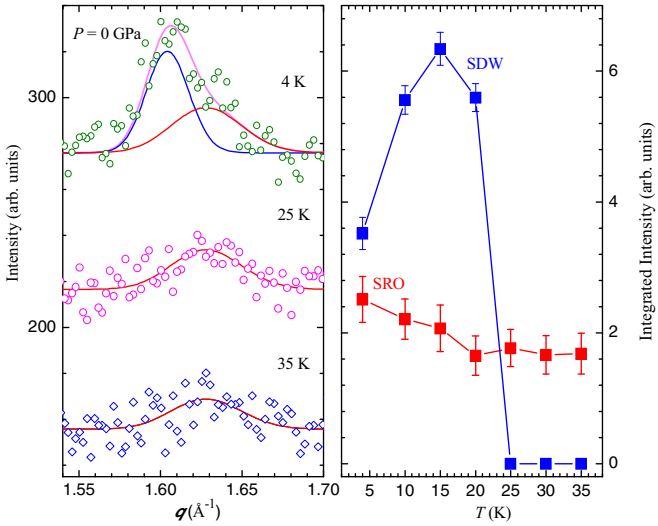

FIG. 5. The sections of the neutron-diffraction patterns in the q space, demonstrating evolution of the peaks associated with the long-range SDW and short-range magnetic order (left) and temperature dependences of their intensities (right). The neighboring patterns are shifted along the vertical axis by 60 units.

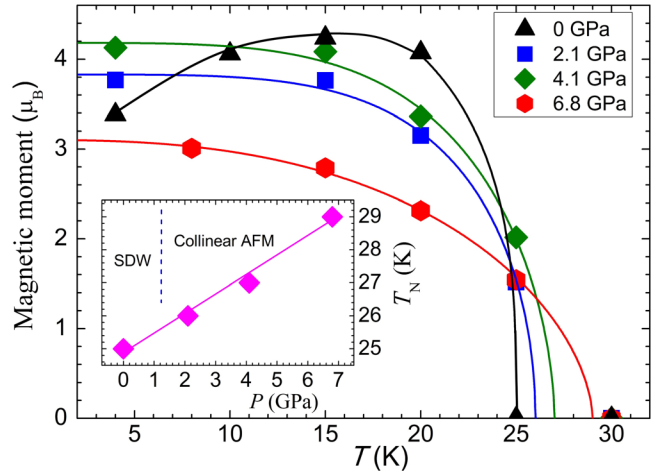

FIG. 6. Temperature dependencies of the ordered Co2 magnetic moment at selected pressures. For $P = 0$ GPa, the line is a guide to the eye only. At high pressures, the solid lines represent interpolations by functions $m = m_0[1 - (T/T_N)^{\alpha}]^{\beta}$. The obtained coefficient values $\alpha \approx 3.5 - 3.0$ and $\beta \approx 0.43 - 0.56$ in the pressure range 2.1–6.8 GPa, respectively. Inset: Pressure dependence of the Néel temperature and its linear interpolation.

One should note that the positions of the peaks characteristic for the suppressed SDW phase are close to several ones of the commensurate AFM phase. Therefore, a presence of the minority regions of the SDW phase at high pressure could not be excluded unambiguously. Further experiments with single-crystal samples would be helpful to clarify this point. No features characteristic for the presence of the short-range magnetically ordered phase were observed in the high-pressure neutron-diffraction data. Disappearance of the anomalous temperature behavior of the ordered magnetic moments at high pressure also points to a suppression of the short-range magnetically ordered phase.

The collinear AFM phase remains stable in the whole studied pressure range up to 6.8 GPa. Its Néel temperature, $T_{NC} = 26(2)$ K at $P = 2.1$ GPa, evaluated from the temperature dependence of the ordered magnetic moment (Fig. 6), is comparable with that for the SDW phase ($T_N = 25$ K). It increases slowly upon compression up to 29 K at 6.8 GPa with a pressure coefficient $dT_N/dP \approx 0.65$ K/GPa (Fig. 6). The ordered magnetic moment values at $T = 4$ K and pressures 2.1–4.1 GPa, $m_{Co2} = 3.8(1) - 4.1(1)\mu_B$ remain close to the spin-only value. At higher pressure $P = 6.8$ GPa a reduction of m_{Co2} to $3.0(1)\mu_B$ occurs. Similar behavior was also observed in the low-dimensional antiferromagnets $YMnO_3$ and $RbFe(MoO_4)_2$ and it may be attributed to the enhanced magnetic disorder on the geometrically frustrated triangular lattice [33,34].

The complex magnetic order in $Ca_3Co_2O_6$ is formed due to competing character of the major intrachain ferromagnetic interactions (J_1) between Co2 ions in the HS state by means of direct exchange with the intermediate Co1 ion in the LS state and weak interchain super-superexchange interactions Co2-O-O-Co2 between the next-nearest-neighbor Co ions located at the distances about 5.50 (J_2) and 6.25 Å (J_3), respectively (Fig. 1). A role of the configurational magnetic entropy is also considered to be important for a stabilization of the SDW phase [18].

According to the theoretical analysis [10,35], the strength of the intrachain FM interactions is determined by the transfer integral between the Co2(HS) and Co1(LS) ions, $J_1 \sim t_{dd}^4$. From the experimentally determined pressure behavior of the Co1-Co2 distances (Fig. 7) and the distance relationship [36] $t_{dd} \sim (d_{Co1\text{-}Co2})^{-5}$, one can evaluate that the J_1 value increases by 25% upon compression up to 6.8 GPa (Fig. 7). The average strength of the interchain interactions $J_{23} = (J_2 + J_3)/2$ is related to the transfer integrals between the Co2(HS)-O ions and O-O ions as $J_{23} \sim t_{pd}^4 t_{pp}^2$ [37]. Taking into account the experimental pressure dependencies of the Co2-O and O-O distances (Fig. 7) and relationships [34] $t_{pd} \sim (d_{Co2-O})^{-7/2}$ and $t_{pp} \sim (d_{O-O})^{-2}$, one can find the increase of the J_{23} value by 23% in the pressure range 0–6.8 GPa. One should also note that the values of the interatomic Co2-O-O angles, corresponding to the J_2 and J_3 interactions [$\varphi_{Co2\text{-}O\text{-}O} \approx$

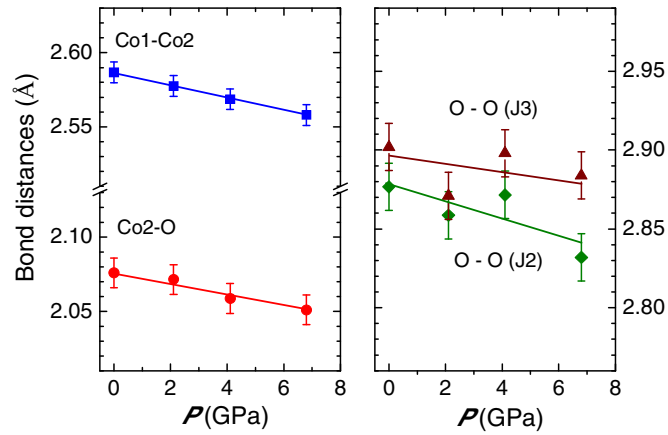

FIG. 7. The pressure dependences of Co1-Co2, Co2-O, and O-O distances.

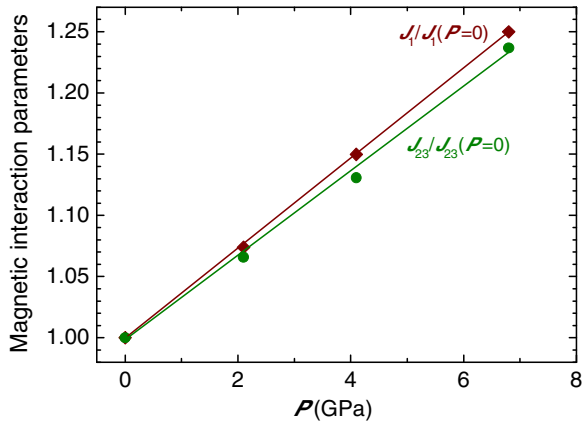

FIG. 8. The pressure evolution of the absolute values of the J_1 and J_{23} magnetic interaction parameters normalized by the ambient pressure values. The error bars do not exceed the symbol sizes (as evaluated from a combination of XRD and neutron-diffraction data).

101.2(5) and 134.9(5)°, respectively], remain about the same in the considered pressure range and their contribution to the modification of magnetic interactions can be neglected. The estimated raising of the J_{23} parameter is also in good agreement with the pressure-induced modification of the spin-flip magnetic field ($d\ln H_{SF}/dP \approx 0.04$ GPa^{-1}), directly related to the change of the interchain magnetic interactions strength in $Ca_3Co_2O_6$, which was determined in more restricted range up to 1.2 GPa from magnetic properties measurements [38].

Our estimations show that the J_{23}/J_1 ratio exhibits a tendency towards decrease in the studied pressure range (Fig. 8), leading to suppression of the SDW phase and stabilization of the commensurate AFM phase in $Ca_3Co_2O_6$ under pressure. According to the theoretical considerations [18,39,40], the stability of the incommensurate and commensurate magnetic phases in the magnetic phase diagram of the system of one-dimensional magnetic chains on the triangular lattice is controlled by the ratio of the inter- and intrachain interaction strengths J_{23}/J_1 and its decrease makes the commensurate antiferromagnetic order more favorable.

The pressure evolution of the Néel temperature of the pressure-induced collinear AFM phase can be evaluated using the analytical solutions for the static susceptibility of the one-dimensional Ising model within the mean field approach [12]:

$$\chi(T) = (1/k_B T)\frac{1}{\cosh\left(\frac{2J_1}{k_B T}\right)}\frac{1}{1-\tanh\left(\frac{2J_1}{k_B T}\right)}, \quad (2)$$

$$\chi^{-1}(T_{NC}) = -2(J_2 + J_3) = -4J_{23}. \quad (3)$$

Taking the ambient pressure values $J_1 = 23.9$ K and $J_{23} = -1.15$ K from Ref. [12] and using the pressure dependences of these parameters evaluated from the experimental data (Fig. 8), one may calculate the pressure coefficient $dT_{NC}/dP \approx 0.85$ K/GPa, well comparable with the experimental value of 0.65 K/GPa.

One should also note that high-pressure effects on the magnetic order of $Ca_3Co_2O_6$ are drastically different from those of chemical substitution. In the $Ca_3Co_{2-x}Fe_xO_6$ compounds ($x = 0.2 - 0.4$), a coexistence of the SDW long-range ordered and the short-range ordered magnetic states was revealed, with a weak temperature and time-dependent volume fractions [41]. The Néel temperature was reduced upon Fe doping to $T_N = 17$ K($x = 0.4$). In the $Ca_{2.75}R_{0.25}Co_2O_6$ compounds (R = Dy, Lu), the rare-earth substitution leads to a stabilization of the SDW phase with $T_N = 17$ K [42]. The observed effects were related to a reduction of the intrachain magnetic interactions, caused by either Fe substitution or enlargement of Co-Co distances in the spin chains due to R element substitution.

IV. CONCLUSIONS

The present results demonstrate that the symmetry of the long-range magnetic order in the quasi-one-dimensional spin-chain compound $Ca_3Co_2O_6$ is highly sensitive to application of high pressure. The lattice compression leads to a suppression of the spin-density wave magnetic phase and stabilization of the collinear commensurate antiferromagnetic phase. The role of the competing intra- and interchain magnetic interactions mediated by variation of interatomic distances has been analyzed, pointing to more significant increase of intrachain ones upon compression. The subsequent reduction of the J_{23}/J_1 magnetic interaction parameters ratio is a possible reason for the observed pressure-induced magnetic phase transformation. The evolution of the Néel temperature of the pressure-induced AFM phase was analyzed in the framework of the mean field theory approach for the one-dimensional Ising model and a good agreement with the experimental value was obtained.

ACKNOWLEDGMENTS

The work has been supported by the Russian Foundation for Basic Research, Grant No. 18-02-00359-a and the Vietnam National Foundation for Science and Technology Development (NAFOSTED) under Grant No. 103.02-2017.364. M.H.P. and H.S. acknowledge support from the U.S. Department of Energy, Office of Basic Energy Sciences, Division of Materials Sciences and Engineering under Award No. DE-FG02-07ER46438. Portions of this research were carried out at the light source PETRA III at DESY, a member of the Helmholtz Association (HGF).

[1] S. Sachdev, *Quantum Phase Transitions* (Cambridge University, Cambridge, England, 2011).
[2] Ch. Rüegg, N. Cavadini, A. Furrer, H.-U. Güdel, K. Krämer, H. Mutka, A. Wildes, K. Habicht, and P. Vorderwisch, Nature (London) **423**, 62 (2003).
[3] F. D. M. Haldane, Phys. Rev. Lett. **50**, 1153 (1983).
[4] S. Maslov and A. Zheludev, Phys. Rev. B **57**, 68 (1998).
[5] M. Pregelj, A. Zorko, O. Zaharko, H. Nojiri, H. Berger, L. C. Chapon, and D. Arčon, Nature Commun. **6**, 7255 (2015).

[6] W. Shiramura, K. Takatsu, B. Kurniawan, H. Tanaka, H. Uekusa, Y. Ohashi, K. Takizawa, H. Mitamura, and T. Goto, J. Phys. Soc. Jpn. **67**, 1548 (1998).

[7] M. Oshikawa, M. Yamanaka, and I. Affleck, Phys. Rev. Lett. **78**, 1984 (1997).

[8] T. Basu, V. V. R. Kishore, S. Gohil, K. Singh, N. Mohapatra, S. Bhattacharjee, B. Gonde, M. P. Lalla, P. Mahadevan, S. Ghosh, and E. V. Sampathkumaran, Sci. Rep. **4**, 5636 (2014).

[9] H. Fjellvåg, E. Gulbrandsen, S. Aasland, A. Olsen, and B. C. Hauback, J. Solid State Chem. **124**, 190 (1996).

[10] R. Frésard, C. Laschinger, T. Kopp, and V. Eyert, Phys. Rev. B **69**, 140405 (2004).

[11] Y. Kamiya and C. D. Batista, Phys. Rev. Lett. **109**, 067204 (2012).

[12] G. Allodi, P. Santini, S. Carretta, S. Agrestini, C. Mazzoli, A. Bombardi, M. R. Lees, and R. De Renzi, Phys. Rev. B **89**, 104401 (2014).

[13] S. Aasland, H. Fjellvåg, and B. Hauback, Solid State Communications **101**, 187 (1997).

[14] H. Kageyama, K. Yoshimura, K. Kosuge, X. Xu, and S. Kawano, J. Phys. Soc. Jpn. **67**, 357 (1998).

[15] O. A. Petrenko, J. Wooldridge, M. R. Lees, P. Manuel, and V. Hardy, Eur. Phys. J. B **47**, 79 (2005).

[16] S. Agrestini, C. L. Fleck, L. C. Chapon, C. Mazzoli, A. Bombardi, M. R. Lees, and O. A. Petrenko, Phys. Rev. Lett. **106**, 197204 (2011).

[17] J. A. M. Paddison, S. Agrestini, M. R. Lees, C. L. Fleck, P. P. Deen, A. L. Goodwin, J. R. Stewart, and O. A. Petrenko, Phys. Rev. B **90**, 014411 (2014).

[18] L. C. Chapon, Phys. Rev. B **80**, 172405 (2009).

[19] P. Lampen, N. S. Bingham, M. H. Phan, H. Srikanth, H. T. Yi, and S. W. Cheong, Phys. Rev. B **89**, 144414 (2014).

[20] V. Hardy, M. R. Lees, O. A. Petrenko, D. McK. Paul, D. Flahaut, S. Hébert, and A. Maignan, Phys. Rev. B **70**, 064424 (2004).

[21] T. Basu. K. K. Iyer, K. Singh, and E. V. Sampathkumaran, Sci. Rep. **3**, 3104 (2013).

[22] Y. J. Choi, H. T. Yi, S. Lee, Q. Huang, V. Kiryukhin, and S.-W. Cheong, Phys. Rev. Lett. **100**, 047601 (2008).

[23] Paula J. Lampen Kelley, Ph.D. dissertation, University of South Florida, 2015, http://scholarcommons.usf.edu/etd/5874.

[24] H.-P. Liermann, W. Morgenroth, A. Ehnes, A. Berghäuser, B. Winkler, H. Franz, and E. Weckert, J. Phys.: Conf. Ser. **215**, 012029 (2010).

[25] N. A. Dubrovinskaia and L. S. Dubrovinsky, Rev. Sci. Instrum. **74**, 3433 (2003).

[26] A. P. Hammersley, S. O. Svensson, M. Hanfland, A. N. Fitch, and D. Hausermann, High Press. Res. **14**, 235 (1996).

[27] V. L. Aksenov, A. M. Balagurov, V. P. Glazkov, D. P. Kozlenko, I. V. Naumov, B. N. Savenko, D. V. Sheptyakov, V. A. Somenkov, A. P. Bulkin, V. A. Kudryashev, and V. A. Trounov, Physica B **265**, 258 (1999).

[28] V. P. Glazkov and I. N. Goncharenko, Fizika i Technika Vysokih Davlenij **1**, 56 (1991) (in Russian).

[29] J. Rodríguez-Carvajal, Physica B **192**, 55 (1993).

[30] F. J. Birch, J. Geophys. Res. **91**, 4949 (1986).

[31] D. P. Kozlenko, N. O. Golosova, Z. Jirák, L. S. Dubrovinsky, B. N. Savenko, M. G. Tucker, Y. Le Godec, and V. P. Glazkov, Phys. Rev. B **75**, 064422 (2007).

[32] S. Agrestini, L. C. Chapon, A. Daoud-Aladine, J. Schefer, A. Gukasov, C. Mazzoli, M. R. Lees, and O. A. Petrenko, Phys. Rev. Lett. **101**, 097207 (2008).

[33] D. P. Kozlenko, I. Mirebeau, J.-G. Park, I. N. Goncharenko, S. Lee, J. Park, and B. N. Savenko, Phys. Rev. B **78**, 054401 (2008).

[34] D. P. Kozlenko, S. E. Kichanov, E. V. Lukin, N. T. Dang, L. S. Dubrovinsky, E. A. Bykova, K. V. Kamenev, H.-P. Liermann, W. Morgenroth, A. Ya. Shapiro, and B. N. Savenko, Phys. Rev. B **87**, 014112 (2013).

[35] C. Laschinger, T. Kopp, V. Eyert, and R. Frésard, J. Magn. Magn. Mater. **272–276**, 974 (2004).

[36] W. A. Harrison, *Electronic Structure and the Properties of Solids* (Dover, New York, 1989).

[37] S. Tornow, O. Entin-Wohlman, and A. Aharony, Phys. Rev. B **60**, 10206 (1999).

[38] B. Martínez, V. Laukhin, M. Hernando, J. Fontcuberta, M. Parras, and J. M. González-Calbet, Phys. Rev. B **64**, 012417 (2001).

[39] Zheng Weihong, R. H. McKenzie, and R. P. Singh, Phys. Rev. B **59**, 14367 (1999).

[40] S. Rao and D. Sen, J. Phys.: Condensed Matter **9**, 1831 (1997).

[41] A. Jain and S. M. Yusuf, Phys. Rev. B **83**, 184425 (2011).

[42] A. Jain, S. M. Yusuf, S. S. Meena, and C. Ritter, Phys. Rev. B **87**, 094411 (2013).